BULLETIN OF THE POLISH ACADEMY OF SCIENCES
TECHNICAL SCIENCES, Vol. 68, No. 3, 2020
DOI: 10.24425/bpasts.2020.133123

Optimized fractional low and highpass filters of $(1 + \alpha)$ order on FPAA

N. SINGH[1]*, U. MEHTA[2], K. KOTHARI[2], and M. CIRRINCIONE[2]

[1] School of Engineering and Physics, University of the South Pacific, Laucala, Suva, Fiji, now at SPARC Hub Headquarters, 71 Normanby Rd, Notting Hill VIC 3168, Australia

[2] School of Engineering and Physics, University of the South Pacific, Laucala, Suva, Fiji

Abstract. This work proposes an optimum design and implementation of fractional-order Butterworth filter of order $(1 + \alpha)$, with the help of analog reconfigurable field-programmable analog array (FPAA). The designed filter coefficients are obtained after dual constraint optimization to balance the tradeoffs between magnitude error and stability margin together. The resulting filter ensures better robustness with less sensitivity to parameter variation and minimum least square error (LSE) in magnitude responses, passband and stopband errors as well as a better –3 dB normalized frequency approximation at 1 rad/s and a stability margin. Finally, experimental results have shown both lowpass and highpass fractional step values. The FPAA-configured outputs represent the possibility to implement the real-time fractional filter behavior with close approximation to the theoretical design.

Key words: fractional-order filter, FPAA, realization, robustness, bilevel optimization.

1. Introduction

Fractional calculus (FC) has been seen as more generalized than the traditional integer calculus, manifesting the potential to accomplish what integer calculus cannot [1]. Recently, it is being applied in many fields of science and technology such as engineering, biomedicine, control theory, diffusion theory, material science, robotics and signal processing [1–3]. The FC applied to signal processing and circuit theory has shown more potential. For example, FC has been imported to electronics, making it possible to design and realize fractional order filter circuits [4]. Well known analog filters contain inductors and capacitors whose numbers determine the filter order. However, an inductor or capacitor with fractional impedance can be generalized and these elements in the fractional domain are called fractance devices [5, 6]. Fractance devices are not available commercially, however it is possible to emulate them using resistor-capacitor (RC) or resistor-inductor-capacitor (RLC) trees and using platforms such as the field-programmable analog array (FPAA). In order to realize fractance devices physically for fractional order circuits and systems, s^{α} is used (where $\alpha \in \mathbb{R}$). This fractional Laplacian operator (FLO) is a multi-valued expression with an infinite number of Riemann surfaces. When constraining s^{α} by imposing integer-order approximations, a transfer function is described using several definitions available, such as those provided by like Riemann-Liouville (R-L), Caputo, Weyl and Grunwald-Letnikov (G-L). In this work, an R-L definition is used, based on Euler's gamma function.

At first, fractional-order filters (FOF) were critically studied in [7] and shown that fractional filters (also called fractional-step filters) are realizable with reasonable overshoot in the passband region. In most cases α ranges from 0.1 to 0.9. Since, as is well known, any second-order filter transfer function leads to a resonant peak in the magnitude response, the magnitude response of the fractional-order Butterworth filter has been explored to address this [4, 8]. The same concept has also been used for elliptical and Chebyshev filters [9, 10]. More recently, Kubanek and Freeborn [11] have proposed a new fractional-order low-pass filter (FLPF) design focussing on the search for coefficients to approximate a second order lowpass filter transfer function with arbitrary quality factor Q. In [10] and [12], coefficients of FLPF transfer function were selected to approximate a flat passband response of a first order Butterworth filter. Another method was proposed in [13] to approximate coefficients for different cases of a normalized FLPF transfer function, but this method was based on limited search for objective functions, and focused on only few parameters, such as transition bandwidth and maximum allowable peak.

Many works have recently been completed on obtaining filter parameters through optimization subroutines. Mahata et al. in [13] have used a nature-inspired optimization subroutine called the gravitational search algorithm (GSA) to optimize parameters of the $(1 + \alpha)$ order transfer function. In this method, authors have presented an approximation of FLO using third order transfer function instead of second order transfer function. In another recent work, a second order approximation of FLO has been used to design a fractional-order low pass Butterworth filter [15]. It was developed using CMOS of the differential difference current conveyor, which was fabricated in a CMOS processor. The benefit of this particular filter was that it allowed low voltage operation within ±500 mV. An

*e-mail: nikhil.singh1@monash.edu

Manuscript submitted 2019-11-05, revised 2020-01-21, initially accepted for publication 2020-02-16, published in June 2020

electronically reconfigurable fractional-order filter has been designed in a recent work that can be configured to work as either FLPF or FHPF [16].

In particular, [12] shows that FOF can provide precise control of attenuation, i.e. –3 dB frequency and stopband attenuation. Integer-order filters yield $-20n$ dB/decade stopband attenuations, where n is the integer order, however fractional order provides greater control with $-20(n+\alpha)$ dB/decade stopband attenuation, where α is any real positive value less than 1 [12, 17]. Basically the $(n+\alpha)$ FOF can give more precise control of the attenuation slope by an additional degree of freedom as compared to integer-order filters of order n. Band pass and band reject filters with asymmetric stopband characteristics [18] can be easily implemented using FOF and can be used as phase discriminators.

However, there are some challenges to obtain the optimum coefficients of the fractional-order transfer function (FOTF). It is desired to select filter coefficients which are optimum for any real differential orders while providing greater robustness. Indeed, variation in coefficients may affect the –3 dB frequency, stopband attenuation and stability. In this work, the coefficient and real value differential orders are computed so that the desired characteristic can be always maintained even if the parameters vary from the designed value. Firstly, the optimized values of the filter are calculated with the help of modified particle-swarm-optimization (PSO) in order to satisfy the constraint requirements. Compared to other optimization routines, the advantages of the PSO are that it is easy to implement with few parameters needing adjustment. The performance of the new fractional-step filters has been verified. Secondly, the optimum order of approximation s^{α} is proposed in order to implement the fractional differentiator in hardware with acceptable accuracy, and the resulting filter is implemented in the Anadigm development environment of FPAA. The waveforms from both the proposed lowpass filter (LPF) and highpass filter (HPF) are measured with various ranges of signal input frequencies. The performance of non-integer filters of order $(1+\alpha)$ has been studied and compared with corresponding integer filters through both experimentation and simulation. The obtained results confirm that the actual fractional filter's behavior closely follows the theoretical approximations for all values of α. Table 1 shows the comparison of previous work in terms of design approach mapped with benefits.

2. Fractional transfer functions of $(1+\alpha)$ order

2.1. LPF transfer function of $(1+\alpha)$ order. The FLPF transfer function of the $(1+\alpha)$ order has previously been studied in [10–12]. Most works focused on the design and implementation of FOTF in the following form:

$$H_{1+\alpha}^{LP} = \frac{k_1}{s^{1+\alpha} + s^{\alpha}k_2 + k_3}, \quad 0 \le \alpha \le 1. \tag{1}$$

The coefficients k_2 and k_3 are selected to yield a flat passband response while k_1 is usually kept at the constant value of 1, which leads to a DC gain of $1/k_3$. Any filter realization is evaluated based on a flat passband with minimum error in magnitudes in the passband and stopband frequencies and with –3 dB normalized frequency almost close to 1 rad/s. This is achieved by minimizing the error objective function with the ideal normalized first order Butterworth response.

Freeborn et al. [10] have optimized the coefficients in (1) through a least squares error (LSE) approach that compared the response with a first order Butterworth response over the normalized frequency range of $\omega = 0.01 - 1$ rad/s. The obtained coefficients yield the minimum cumulative passband error. The numerical search is limited to $0 < k_2 < 2$, $0 < k_3 < 1$ and $k_1 = 1$. Another attempt was presented using the MATLAB optimization tool based on a nonlinear least squares fitting [12], where the improved LSE comes at the cost of the stability margin. Thus the trade-offs between LSE and stability margin are hard to be guaranteed in a uniform way against different design objectives. Because of the above difficulties, any optimization technique should be multi-objective.

In this work, modified particle swarm optimization (mPSO) has been developed to work with more than two objectives at a time. Main focus is on the design of an optimum FOTF so that the uniformity of the trade-offs between LSE and the stability margin can be guaranteed. Although the computational complexity of the problem is further increased by the bilevel structure, the desired solution can be achieved in a finite time. In this paper, the novelty lies in the fact that the filter designed satisfies more than one characteristic at the same time. An objective function has been developed that gives the minimum of the magnitude error, with flat passband response, –3 dB

Table 1
Summary of design approaches and benefits

Design approach	Benefits
Coefficient search to approximate TF with arbitrary Q [11]	Greater stability and higher degree of freedom for coeffiecient variation
Coefficients selected to approximate flat passband response [12]	Minimum passband error and higher stability
GSA used to optimize transfer function coefficients [14]	Third order transfer function is used to approximate Butterworth response using FLO
Proposed design approach using PSO	The proposed filter ensures better robustness with less sensitivity to parameter variation, minimum least square error (LSE) in magnitude responses, passband and stopband errors as well as a better –3 dB normalized frequency approximation at 1 rad/s, and a stability margin

frequency reached at 1 rad/s. The proposed algorithm solves a two-step problem of the so-called bilevel ptimization routine. Further, the simulated $(1+\alpha)$ order LPFs with fractional steps from $\alpha = 0.01$ to $\alpha = 0.99$ have been developed and analyzed statistically. The results are compared with the existing FOF reported in recent literature. In the following section, the modified mPSO with selected coefficients is presented. The advantage of global search and the optimum robust result findings feature of mPSO are investigated in this analysis.

2.2. mPSO for bilevel optimization. It is necessary to choose the best filter parameters to meet the design requirements and then these selected values can be used to implement the fractional filter on the reconfigurable platform. Indeed [19] shows that the basic PSO is computationally less expensive and has lower memory requirements than other optimization routines. In addition, it has a relatively small number (3 to 5) of user-defined parameters, which are not critical for the convergence and final accuracy of the algorithm. It is also suitable for solving continuous nonlinear optimization problems. The basic PSO version with inertia weight is described in the formula below [20].

$$\begin{aligned} a_i &\leftarrow \Omega a_i + R(0, \varphi_1) \otimes (p_i - x_i) + \\ &\quad + R(0, \varphi_2) \otimes (p_g - x_i), \\ x_i &\leftarrow x_i + a_i \end{aligned} \tag{2}$$

where $i \in N$, Ω is an inertia weight factor which determines speed of the particle, N is the number of particles (usually $N <= 40$) and $\otimes$ is the Kronecker multiplication; x_i gives the particle's actual location and a_i defines the step velocity of the particle. The parameters φ_1 and φ_2 (acceleration coefficients) determine the magnitude of the random forces in the direction of best particle p_i and the neighborhood best p_g. $R(0, \varphi_j)$, $(j = 1, 2)$ delivers a vector of random numbers uniformly distributed in $[0, \varphi_j]$, after each iteration and for each particle. The inertia weight factor Ω is updated by the following law:

$$\Omega = \Omega_{\max} - (I_k - 1)\left(\frac{\Omega_{\max} - \Omega_{\min}}{I_m - 1}\right) \tag{3}$$

in which $\Omega_{\max}$ and $\Omega_{\min}$ are maximum and minimum inertia weights, respectively, I_k is the current iteration and I_m is the maximum iteration number. Table 2 shows the parameter values used in this work.

Table 2
mPSO parameters

Parameters	N	$\Omega_{\min}$	$\Omega_{\max}$	I_m	φ_1	φ_2
Value	35	0.1	0.9	100	1	2

In the implementation proposed, we have modified the boundary conditions and this constraints user settings. We concider this algorithm as mPSO. When a given boundary is violated by any of the particles, this particle i is returned to its previous position x_i. In this scenario, mPSO will reverse the step (a_i) in the opposite direction (i.e. $a_i = -a_i$). In this work, k_2 and k_3 of (1) are fed in as the variables to be optimized. The optimization is carried out with the following bilevel objectives in order to balance the tradeoffs between LSE and –3 dB variation close to the normalized frequency of 1 rad/s.

Level 1: The minimum LSE, calculated as

$$E_c(j\omega) = \sum_{i=1}^{N} \left| \left|B_1(j\omega_i)\right| - \left|H_{1+\alpha}^{LP}(j\omega_i)\right| \right|^2 \tag{4}$$

where E_c is the cumulative error and the magnitude responses $\left|B_1(j\omega)\right|$ and $\left|H_{1+\alpha}^{LP}(j\omega)\right|$ are the first order Butterworth filter and the fractional order LPF of order $(1+\alpha)$ at pulsation ω_i, respectively, and N is the number of samples taken between frequency 0.01–1.5 rad/s.

Level 2: –3 dB frequency closest to 1 rad/s minimization of:

$$(\omega_{3dB} - 1)^2. \tag{5}$$

The proposed mPSO with constraints in (4) and (5) and the optimum set of coefficients were obtained for all $(1+\alpha)$ order transfer functions. The linear curve-fitted expressions (6, 7) were obtained in terms of parabolic function of order 3 and as a function of α as follows.

$$k_2{}^{proposed} = 0.5293\alpha^3 - 0.3156\alpha^2 + 0.9672\alpha + 0.2653 \tag{6}$$

$$k_3{}^{proposed} = -0.1981\alpha^3 + 0.2471\alpha^2 + 0.2359\alpha + 0.7233 \tag{7}$$

The coefficients k_2 and k_3 that yielded the best performance for (1) with $k_1 = 1$, when the order is increased from 1.01 to 1.99 in steps of 0.01, are described and compared in Fig. 1.

2.3. HPF transfer function of $(1+\alpha)$ order. An FHPF can also be obtained from the FLPF transfer function by means of the transformation highlighted in [21]. There are three different transformations, each of which has its own pros and cons. In the previous section, coefficients of FLPF (1) were chosen

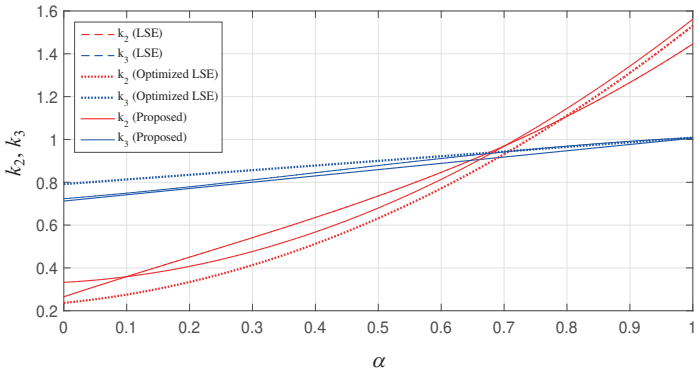

Fig. 1. Comparison of k_2 and k_3 coefficients to approximate fractional step filters: proposed, LSE [10], optimized LSE [12]

using bilevel mPSO and provided a maximally flat passband response, minimum stopband and passband errors and –3 dB frequency close to or equal to 1 rad/s. In the same manner, the transformation provided minimum passband and stopband errors for the HPF when the proposed coefficients were chosen from the previous subsection. It is noteworthy that this HPF transfer function is obtained just by replacing the Laplacian operator s by $1/s$ which results in (1) to become:

$$H_{1+\alpha}^{HP3}(s) = \frac{s^{1+\alpha}k_1}{s^{1+\alpha}k_3 + sk_2 + 1}. \tag{8}$$

The unity value of coefficient k_1 provides a passband gain of $1/k_3$ in (8). By comparing (1) and (8), an interchange of denominator coefficients is present in (8) for the coefficient of middle term k_2. The term s^α in (1) has been replaced by s in (8). At the frequency of 1 rad/sec, this lowpass to highpass transformation provides the same response characteristics.

3. Numerical comparison and examination with fixed parameters

A detailed error analysis, stability analysis and sensitivity to parameter variation are performed in the following subsection, comparing the performance of the proposed filter coefficients with those presented in [12] and [10].

3.1. LPF evaluation. The FLPF offers stopband attenuations of $-20(1+\alpha)$ dB per decade. The proposed filter performance is analysed after calculating the coefficients, in terms of passband error, stopband error, stability, –3 dB frequency and sensitivity to parameter variation.

3.1.1. Magnitude response error. It has been evaluated by using mean square error (*MSE*) given by (9)

$$MSE = \sqrt{\frac{\sum_{i=1}^{M}\left|\left|H_{B1}(\omega_i)\right| - \left|H_{1+\alpha}^{LP}(\omega_i)\right|\right|^2}{M}} \tag{9}$$

where $H_{B1}(\omega_i)$ is the magnitude response of first order Butterworth filter at frequency ω_i for 100,000 samples taken within the frequency range from 0.001 to 100 rad/s. $\left|H_{1+\alpha}^{LP}(\omega_i)\right|$ is the magnitude response of the $(1+\alpha)$ order Butterworth LPF.

The magnitude response performance of the designed filters is also compared based on two error matrices, namely passband error (*PE*) and stopband error (*SE*), defined as following.

$$PE = 20\log_{10}\left\{\sqrt{\frac{\sum_{i=1}^{K}\left|\left|H_{B1}(\omega_i)\right| - \left|H_{1+\alpha}^{LP}(\omega_i)\right|\right|^2}{K}}\right\} dB \tag{10}$$

where, $K = 50{,}000$ and $0.001 \leq \omega \leq 1$.

$$SE = 20\log_{10}\left\{\sqrt{\frac{\sum_{i=1}^{L}\left|\left|H_{B1}(\omega_i)\right| - \left|H_{1+\alpha}^{LP}(\omega_i)\right|\right|^2}{L}}\right\} dB \tag{11}$$

where, $L = 50{,}000$ and $1 \leq \omega \leq 100$.

Both *PE* and *SE* errors of fractional $(1+\alpha)$ order filters are listed, which is calculated using the coefficients used in [10, 12] and proposed coefficients in Table 3. It is also clear from Fig. 2 that the proposed filter would mostly provide the lowest errors for almost all orders of filters, especially for PE. As for the SE values, Fig. 2b gives errors consistent but slightly lower in the range from 1 to 1.9 for $(1+\alpha)$.

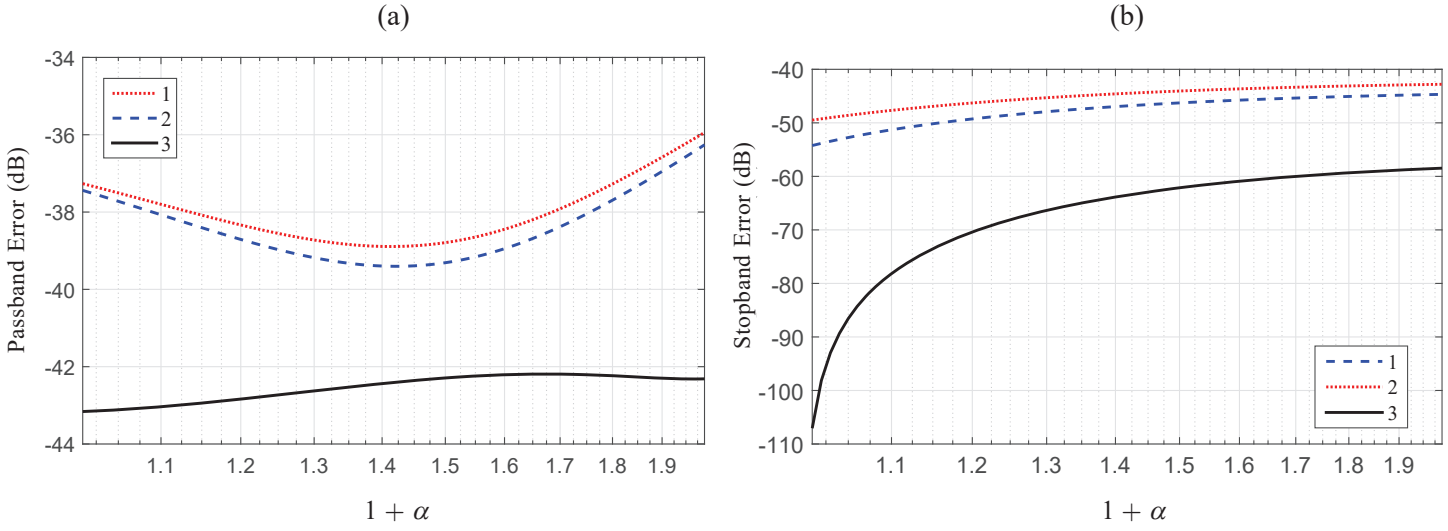

Fig. 2. (a) PE index values: 1. by [10], 2. by [12], 3. proposed; (b) SE index values: 1. by [10], 2. by [12], 3. proposed

Table 3
Comparison of PE and SE matrices for $(1+\alpha)$ order filters

Error	Methods	$1+\alpha$								
		1.1	1.2	1.3	1.4	1.5	1.6	1.7	1.8	1.9
PE (dB)	[10]	–37.80	–38.33	–38.72	–38.90	–38.79	–38.45	–37.92	–37.27	–36.58
	[12]	–38.07	–38.71	–39.18	–39.40	–39.31	–38.95	–38.38	–37.69	–36.95
	Proposed	–43.03	–42.84	–42.63	–42.44	–42.29	–42.21	–42.19	–42.23	–42.30
SE (dB)	[10]	–47.67	46.28	–45.31	–44.59	–44.06	–43.65	–43.34	–43.11	–42.92
	[12]	–51.30	–49.27	–47.92	–46.97	–46.27	–45.76	–45.37	–45.07	–44.84
	Proposed	–78.16	–70.40	–66.37	–63.85	–62.13	–60.90	–60.00	–59.33	–58.87

3.1.2. Stability region analysis. An important criterion to be examined with the proposed optimized coefficients is the stability margin, described in terms of pole angle and the region of instability. To analyze the stability margin of FLPF, let us convert (1) to complex W-plane [22]. The transformation is possible for the common value transfer function and it converts the FOTF to the W-plane by taking $s = W^m$ where $\alpha = l/m$ (l, m are integers selected for the desired α value, if α is a rational number).

This transformation changes (1) into

$$H(W) = \frac{k_1}{W^{m+k} + k_2 W^k + k_3}. \tag{12}$$

The characteristic equation from (12) in W-plane should ensure that all the poles obtained with optimized coefficients are in the stable region. It is necessary to observe further how far the absolute pole angles, $|\theta_W|$, are from the value of $\frac{\pi}{2m}$. If any $|\theta_W| < \frac{\pi}{2m}$, then the system is unstable. The minimum root angles have been calculated for $\alpha = 0.01$–0.99 with $l = 10$ to 990 in steps of 10 while $m = 1000$. First, by equating the denominator of (12) to 0 for all values of α, the absolute values of the minimum angle of the root $\left(|\theta_W|_{\min}\right)$ were calculated and plotted in Fig. 3a. The criterion for stability is $|\theta_W| < \frac{\pi}{2m}$ and according to the chosen l and m, for stability $|\theta_W| < \frac{\pi}{2m} = 0.09°$. The minimum root angle using the proposed coefficients shows a visibly higher margin than others. Interestingly, the optimized coefficients with LSE in [12] yield a lower stability than the proposed method even though their method gives a lower LSE. For $(1+\alpha)$ between 1.2 to 1.8, the minimum root angles are further away from the unstable boundary as compared with coefficients from [12] and [10]. It can be concluded from the results that the proposed design has obtained a better stability margin with a lower value of LSE.

3.1.3. –3 dB frequency analysis. It is desired that the pulsation from the transfer function coefficient be approximately 1 rad/s at –3 dB. Thus for each order from 1.01 to 1.99, the frequency at which the magnitude response reaches –3 dB is compared. According to the criterion, the fractional Butterworth filter that reaches –3 dB below its DC value at the frequency of 1 rad/s is the best choice for implementation. The –3 dB frequencies for each order are given in Fig. 3b and numerically calculated with different sets of coefficients from [10, 12] along with the proposed technique for orders from 1.01 to 1.99 in steps of 0.01. Both coefficients from [10] and [12] show similar deviations

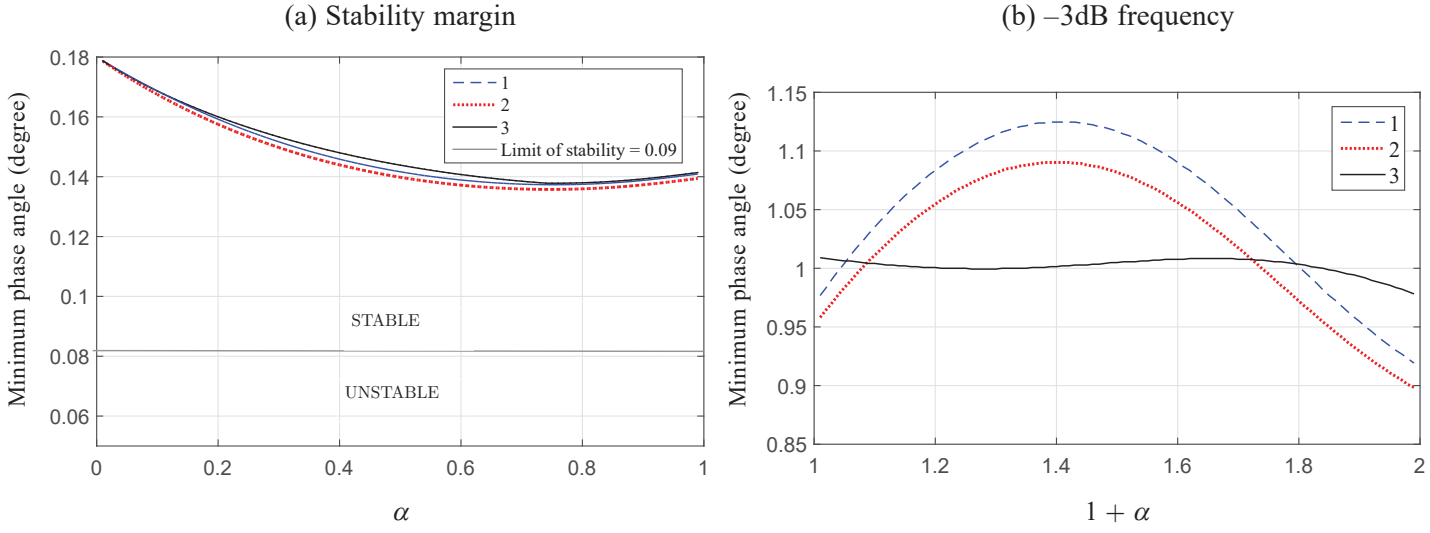

Fig. 3. (a) Stability comparison: 1. by [10], 2. by [12] and 3. proposed; (b) –3 dB frequency comparison: 1. by [10], 2. by [12] and 3. proposed

in –3 dB frequencies and at the order of $1.1 < (1 + \alpha) < 1.5$ frequency increases and reaches the peak of 1.13 rad/s and 1.09 rad/s, respectively. After that, frequency drops gradually and at the 1.8 order it crosses the 1 rad/sec margin in [10] and at 1.7 rad/s in [12]. However, the proposed filter coefficients show the closest agreement to 1 rad/s for all orders. It can be seen that the filter has a lower ripple at –3 dB frequency, fluctuating between 1.005 to 0.998 rad/s. Thus, using bilevel optimization, the desirable filter characteristics can be improved both in the lower LSE value, and with a high stability margin and better –3 dB frequency.

3.1.4. Stopband attenuation. The transfer function (1) has different roll-off characteristics with different sets of coefficients. Stopband attenuation determines how the magnitude response changes from flat passband response to the ideal stopband attenuation of $-20(1 + \alpha)$ dB/decade. Stopband attenuation is another characteristic of the Butterworth response, and the slope of the roll-off characteristics determines the superiority of the design, i.e. the sharper the slope, the better the designed filter.

In order to compare the roll-off characteristics of equation (1) from various methods, the slopes of the magnitude of transfer functions with coefficients from [10, 12] and proposed values are given in Fig. 4. The solid green line is the ideal characteristic of $-20(1 + \alpha)$, changing from a value of –20 dB/decade when $(1 + \alpha) = 1$ to –40 dB/decade when $(1 + \alpha) = 2$; corresponding to the traditional integer-order attenuations available for $\omega = [10, 100]$ rad/s. The slope between frequencies $\omega = 1$ to $\omega = 10$ rad/s is shown with the blue lines and $\omega = 10$ to $\omega =$ rad/s – with red lines for $(1 + \alpha) = 1.01$ to 1.99 in steps of 0.01.The attenuation for all values of α using the proposed approximation shows the roll-off rate closest to the ideal magnitude response for $\omega = 1$ to 10 rad/s as seen in Fig. 4.

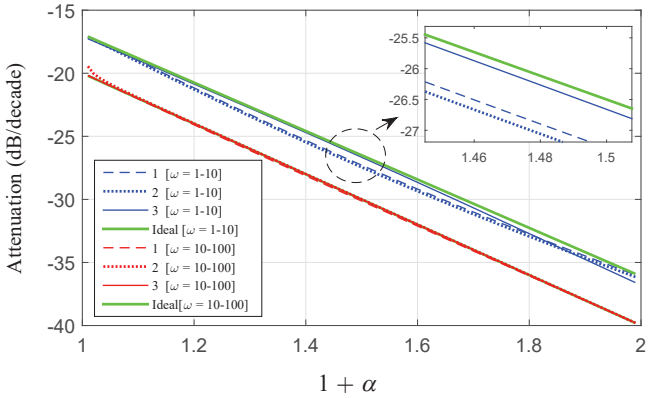

Fig. 4. Stopband attenuation for $(1 + \alpha)$ order Butterworth LPF implementation: 1. by [10], 2. by [12], 3. proposed

3.2. Sensitivity to parameter variation

3.2.1. –3 dB frequency response to parameter variation. The –3 dB frequency for $(1 + \alpha)$ order transfer function (1) with variation in coefficients by a deviation of 1% has been explored in Fig. 5. The result reveals that the best balance among the flat passband and –3db frequency is obtained with the technique proposed. In Fig. 5, both k_2 and k_3 were varied by 1% and for all α varied from 0.1 to 0.9. The coefficients obtained with the proposed method produced the minimum percentage error when compared to [10] and [12]. It can be concluded from the plot that the proposed coefficients are the most suitable ones because the variation in coefficients by (1%) shows the least variation of –3 dB frequencies over the full range of orders.

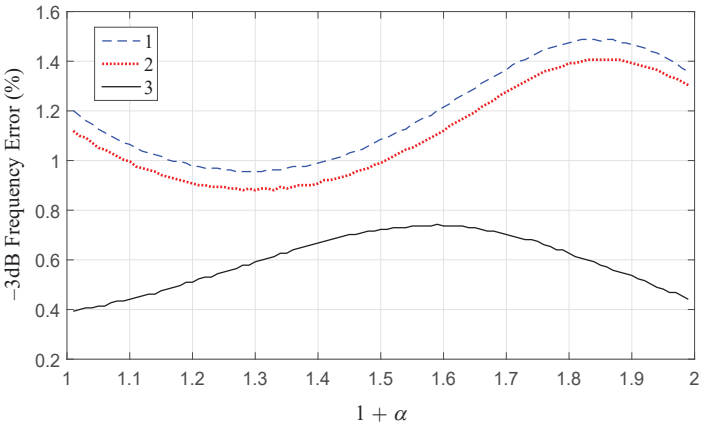

Fig. 5. Percentage error in –3db frequency [k_2 and k_3 varied]: (1) in [10], (2) in [12] and (3) in proposed

3.2.2. Stopband attenuation error to parameter variation. The error in percentage with respect to the ideal attenuation for $(1 + \alpha)$ order transfer function (1) with variation in coefficients by 1% has also been similarly explored and results are shown in Fig. 6. Again the same variations in coefficients are considered as previously; moreover, the effect on attenuation with frequency ranges of $\omega \in [1, 10]$ and $\omega \in [10, 100]$ rad/s are examined. Again, Fig. 6 proves that when both k_2 and k_3 are varied by 1%, the proposed filter is more robust with minimum attenuation error as compared to filters obtained with [10] and [12] methods.

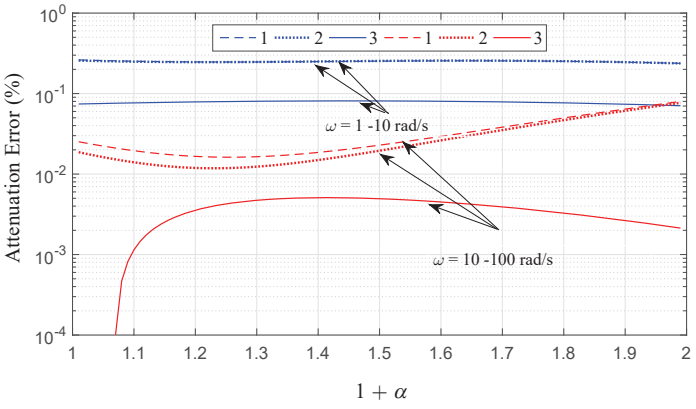

Fig. 6. Percentage error in stopband attenuation [k_2 and k_3 varied]: 1. in [10], 2. in [12], 3. proposed

4. Real-time implementation

In this work, the Anadigm AN231E04 FPAA kit has been configured to test the designed fractional filters. Anadigm FPAA is an 'analog signal processor' consisting of fully configurable analog modules (CAMs) surrounded by programmable interconnect and analogue input and output cells [23]. The CAMs in the FPAA accept transfer functions broken down into pole-zero (PZ) form. In the following section, it is explained briefly how fractional function is converted into the CAMs compatible. There are many advantages of using FPAA that makes it suitable for analog design applications. FPAA works fully in an analog domain, which makes it suitable for many real-world applications. The added benefits include FPAA's low power consumption, high precision, drift free operation, fast processing speed, high level of integration, and the fact that the design can be easily made using PC-based CAD tools. These features make it easier to implement complex filters on FPAA. However, there are some frequency dependent limitations of FPAA. In order to implement filters on the FPAA, a large number of linear switched capacitors is required, which takes up lot of space in the integrated circuit architecture. Moreover, it has operation frequency limitation to the Nyquist rate and also it limits the achievable bandwidth and linearity.

4.1. Approximation of FLO. Approximation for the general FLO [24] can be used to realize fractional order filters. Therefore, one can convert (1) into the following form:

$$H^{LP}_{1+\alpha}(s) = \frac{k_1}{s^{1+\alpha} + k_2 s^{\alpha} + k_3} \cong \cong \frac{k_1(a_2 s^2 + a_1 s + a_0)}{s^3 + c_0 s^2 + c_1 s + c_2} \tag{13}$$

where $a_0 = \alpha^2 + 3\alpha + 2$, $a_1 = 8 - 2\alpha^2$, $a_2 = \alpha^2 - 3\alpha + 2$, $c_0 = (a_1 + a_0 k_2 + a_2 k_3)/a_0$, $c_1 = (a_1(k_2 + k_3) + a_2)/a_0$, and $c_2 = (a_0 k_3 + a_2 k_2)/a_0$. The interpolated equations for coefficients k_2 and k_3 are drawn in Fig. 1, obtained from raw data with the curve fitting function of MATLAB. With these coefficients, both fractional LPF and HPF can be implemented and realized using FPAA, as discussed in the following section.

4.2. $(1 + \alpha)$ order LPF. Previously the implemention of a filter required the determination of the values of the components to realize the transfer functions. Nowadays, however, latest features present in AnadigmDesigner 2 development environment only need the transfer function in the form of PZ frequencies and the quality factor. Accordingly, the transfer function (1) is decomposed into first and second order terms by using the bilinear and biquadratic filter CAM modules. Thus, (1) can be written in the following form:

$$H^{LP}_{1+\alpha}(s) = H_1(s)H_2(s) = \frac{1}{s + d_0} \frac{e_0 s^2 + e_1 s + e_2}{s^2 + 1 d_1 s + d_2}. \tag{14}$$

Two CAMs are used to implement the approximated fractional step filters as shown in (14). The first term $H_1(s)$ is obtained with the bilinear characteristic and the other term $H_2(s)$ – with the biquadratic characteristic. By equating equation (1) with equation (14) the following coefficients can be obtained:

$$\begin{aligned} d_0 + d_1 &= \frac{a_1 + a_0 k_2 + a_2 k_3}{a_0} \\ d_0 d_1 + d_2 &= \frac{a_1(k_2 + k_3) + a_2}{a_0} \\ d_0 d_2 &= \frac{a_0 k_3 + a_2 k_2}{a_0} \\ e_0 = k_1 \frac{a_2}{a_0}, &\quad e_1 = k_1 \frac{a_1}{a_0}, \quad e_2 = k_1. \end{aligned} \tag{15}$$

CAMs have different forms of accepting variables from (14) as specified in the AN231E04 FPAA datasheet [23]. Before transforming (14), the following frequency transformation $s = \left(\frac{s}{\omega_0}\right) = (s/2\pi f_0)$ has to be performed, resulting in:

$$\begin{aligned} H(s) &= T_1(s)T_2(s) \\ T_1(s) &= \frac{2\pi f_1 G_1}{s + 2\pi f_1} \\ T_2(s) &= -\frac{s^2 + \dfrac{2\pi f_{2_z}}{(Q_{2_z})s} + 4\pi^2 {f_{2_z}}^2}{s^2 + \dfrac{2\pi f_{2_z}}{(Q_{2_p})s} + 4\pi^2 {f_{2_p}}^2} \end{aligned} \tag{16}$$

where, T_1 is the transfer function of bilinear CAM, T_2 is the transfer function of biquadratic CAM, G_1 is the gain of T_1, f_1 is the pole frequency of T_1, $f_{2_{p,z}}$ is the PZ frequency of T_2, $Q_{2_{p,z}}$ is the PZ quality factor of T_2 and f_0 is a de-normalized frequency. T_1 and T_2 are implemented using the switched capacitor technology inside the FPAA.

To implement $(1 + \alpha)$ FLPF, the following design equations are to be used from [10].

$$\begin{aligned} f_1 = d_0 f_0, &\quad f_{2_z} = f_0 \sqrt{\frac{e_2}{e_0}}, \quad Q_{2_z} = \frac{\sqrt{e_0 e_2}}{e_1} \\ f_{2_p} = f_0 \sqrt{d_2}, &\quad Q_{2_p} = \frac{\sqrt{d_2}}{d_1}, \quad G_1 = \frac{e_0}{d_0} \end{aligned} \tag{17}$$

The FOLPF of orders $(1 + \alpha) = 1.2, 1.6, 1.9$ have been realized. The approximated PZ frequencies of bilinear and biquadratic CAMs to be realized using Anadigm FPAA are shown in Table 4a when $f_0 = 1$ kHz. Table 4b shows the values of $d_{0,1,2}$ and $e_{0,1,2}$ from (15) used for Table 4a for the same values of α. The values for $k_{2,3}$ in Table 4b are optimized values obtained with the implementation. These values differ from the theoretical values as there are limitations on the values that can be implemented on FPAA. Indeed biquadratic and bilinear CAMs cannot realize all potential values for hardware limitations, since corner frequencies, quality factors and gains are

Table 4
Theoretical and realized biquad and bilinear CAM values for FLPF

(a)

Design parameters	Order $(1+\alpha)$					
	1.2		1.6		1.9	
	Theoretical	Realized	Theoretical	Realized	Theoretical	Realized
f_1, kHz	0.33	0.35	0.46	0.46	0.73	0.73
f_{2_p}, kHz	1.75	1.76	1.48	1.50	1.17	1.18
f_{2_z}, kHz	1.35	1.36	2.72	2.73	7.07	7.11
Q_{2_p}, kHz	0.49	0.49	0.64	0.64	0.67	0.67
Q_{2_z}, kHz	0.24	0.25	0.20	0.21	0.12	0.12
G_1	1.62	1.60	0.28	0.28	0.02	0.02

(b)

value	$(1+\alpha)^{k_2}_{k_3}$		
	$(1+0.2)^{0.46}_{0.78}$	$(1+0.6)^{0.89}_{0.91}$	$(1+0.9)^{1.29}_{0.99}$
d_0	0.33	0.46	0.73
d_1	3.55	2.29	1.73
d_2	3.07	2.21	1.39
e_0	0.54	0.13	0.02
e_1	3.00	1.75	1.15
e_2	1.00	1.00	1.00

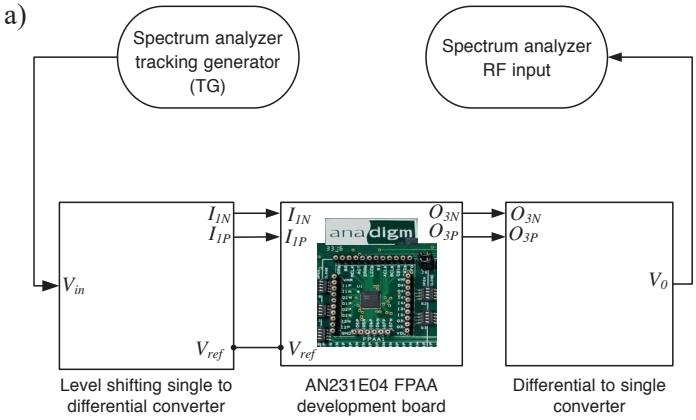

Fig. 7. (a) Block diagram for hardware connection and (b) experimental setup

interrelated with the internal switched capacitor circuits of the FPAA kit. Since the manufacturers only make a finite number of capacitors, the AnadigmDesigner tool selects the best ratio of switched capacitors, matching the desired design parameters. With the coefficients proposed in this paper, the theoretical and realized values are lower than those proposed in [10] and [12] in terms of higher accuracy in passband and stopband values.

4.3. Experimental results for $(1+\alpha)$ order LPF. An FLPF has been implemented on the FPAA development board: the experiment block diagram and the experimental test rig are shown in Fig. 7. The Anadigm FPAA board was powered by 5 V DC, which drew 200 mA of current from the source. The differential-to-single and single-to-differential converters were supplied by 5 V DC supply, each separately, and drew combined current of 250 mA from the supply. The power requirements of the proposed setup ARE similar to that implemented in [10]. The cut-off frequency for the LPF has been set to 1 kHz. The $(1+\alpha)$ order with $\alpha = 0.2$, 0.6 and 0.9 values were implemented. A SSA3000X series spectrum analyser has been used to measure the magnitude response of the implemented LPF. The start frequency has been set to 100 Hz, and the stop frequency to 1 MHz. The tracking generator (TG) level was set as –10 dB. Input voltage signal was generated from the TG source port of the spectrum analyzer at 50 Ω set at 2.7 V, and connected to the input side of the implemented fractional order filter. The output was measured from the RF input port of the spectrum analyzer at 50 Ω. The filter response was recorded on the spectrum analyzer screen. The measured magnitude response of FLPF of order $(1+\alpha) = 0.2$, 0.6 and 0.9 has been recorded.

The magnitude response for $\alpha = 0.2$, 0.6 and 0.9 is shown in Fig. 8, which further confirms the good operation of the proposed FLPF on the FPAA. The extra degree of freedom pro-

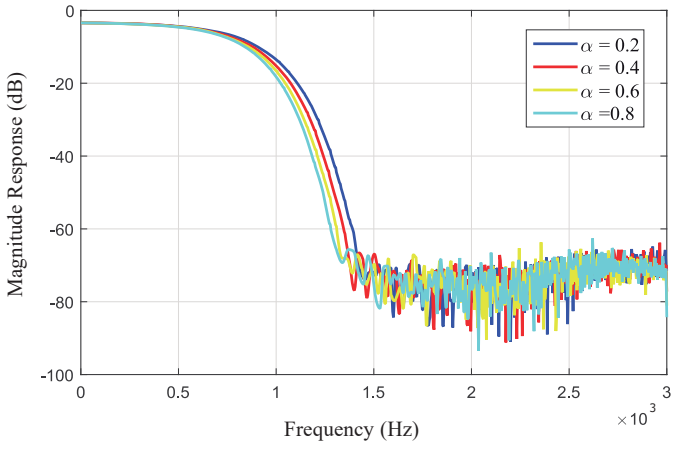

Fig. 8. Real-time fractional $(1+\alpha)$ LPF with orders 1.2, 1.4, 1.6 and 1.8

vided by the fractional order parameter allows the full manipulation of the filter specifications to obtain the desired response required by any application.

4.4. $(1+\alpha)$ order HPF. An FHPF can be implemented in a similar manner by means of decomposition of the transfer function (1) into the form taken in by bi-linear and biquadratic filter CAMS given by (14). The bilinear CAM had input parameters such as corner frequency and gain, and the biquadratic CAM filter had the input parameter in the form of PZ configuration. The design equations for $d_{0,1,2}$ and $e_{0,1,2}$ differ slightly from LPF and can be calculated using the equation set (18).

$$
\begin{aligned}
&p_1 = a_2k_2 + a_0k_3, \quad p_2 = a_1k_2 + a_1k_3 + a_2\\
&p_3 = a_0k_2 + a_2k_3 + a_1, \quad p_4 = a_0\\
&d_0 = \sqrt{\left[(p_1)x^3 - (p_2)x^2 + (p_3)x + p_4\right]}\\
&d_1 = \frac{a_0k_2 + a_2k_3 + a_1}{a_0} - d_0\\
&d_2 = \frac{a_1k_2 + a_1k_3 + a_2}{a_0} - d_0d_1\\
&e_0 = k_1, \quad e_1 = k_1\frac{a_1}{a_0}, \quad e_2 = k_1\frac{a_2}{a_0}.
\end{aligned}
\tag{18}
$$

It is to be noted that x is a dummy variable and d_0 is the positive real root in (18). The values of $k_{2,3}$ that are used to calculate $d_{0,1,2}$ and $e_{0,1,2}$, are proposed coefficients. The values for $d_{0,1,2}$ and $e_{0,1,2}$ for filter orders $(1+\alpha) = 1.2$, 1.6 and 1.9, were calculated using (18), respectively, and are presented in Table 5b along with bilinear and biquadratic filter CAM parameters.

There is not much difference in implementing FHPF on AN231E04 FPAA when compared to FLPF. Both the bilinear and biquadratic filter CAMs are used to implement a highpass. Only the bilinear CAM is set in highpass configuration while earlier it was set to lowpass configuration. The biquadratic filter CAM was not changed and remained the same as the PZ configuration. For HPF $f_0 = 10$ kHz was used as a cut-off frequency. The realized and theoretical values are slightly different due to hardware limitations in implementing high decimal values, as mentioned above.

4.5. Experimental results for $(1+\alpha)$ order HPF. The optimal transformation (8) from fractional order low to highpass filter is used to implement an FHPF. As discussed in an earlier section, the filter was implemented using the best coefficients k_2 and k_3. The cut-off frequency for HPF was set to 10 kHz. Filters of $(1+\alpha)$ orders with $\alpha = 0.2$, 0.6 and 0.9 have been implemented. Frequency range was set up on a 1 kHz to 100 kHz scale. This further confirms the good operation of the proposed FLPF on the FPAA.

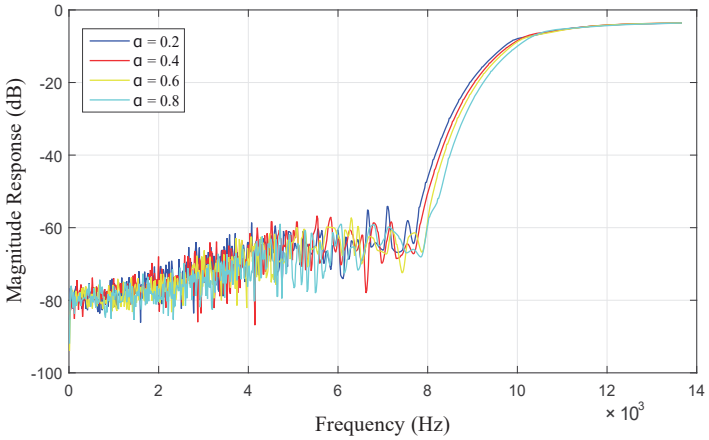

Fig. 9. Real-time fractional $(1+\alpha)$ HPF with orders 1.2, 1.4, 1.6 and 1.8

5. Conclusions

This work has focussed on the design and implementation of fractional order filters, by using a reconfigurable analog processor. The main advantage of this design is that it provides an extra degree of freedom in system designing, and ensures control of passband ripple, roll-off rate, and stopband attenua-

Table 5
Theoretical and realized biquad and bilinear CAM values for FHPF

(a)

Design parameters	Order $(1+\alpha)$					
	1.2		1.6		1.9	
	Theoretical	Realized	Theoretical	Realized	Theoretical	Realized
f_1, kHz	29.83	29.80	21.53	21.50	13.69	13.70
f_{2_p}, kHz	12.59	12.10	14.04	14.00	10.75	10.50
f_{2_z}, kHz	7.38	7.16	3.66	3.83	1.41	1.50
Q_{2_p}, kHz	1.39	1.47	2.30	2.40	0.97	0.98
Q_{2_z}, kHz	0.24	0.25	0.20	0.21	0.12	0.12
G_1	1.00	1.00	1.00	1.00	1.00	1.00

(b)

value	$(1+\alpha)^{k_2}_{k_3}$		
	$(1+0.2)^{0.46}_{0.78}$	$(1+0.6)^{0.89}_{0.91}$	$(1+0.9)^{1.29}_{0.99}$
d_0	2.98	2.15	1.36
d_1	0.90	0.60	1.09
d_2	1.57	1.97	1.15
e_0	1.00	1.00	1.00
e_1	3.00	1.75	1.15
e_2	0.54	0.13	0.02

tion. This can be used in many applications such as designing special controllers, telecommunications and also in modeling of various biological signals. Firstly, a new bilevel constraint optimization was proposed to obtain the best filter parameters. The proposed filters have shown more robustness as compared to previously proposed fractional filters. Through analysis, the optimum order of approximated s^{α} was suggested to implement a fractional differentiator in hardware with acceptable accuracy. The real-time fractional filter has been implemented with the analog array board. The results, obtained with MATLAB and in real time, have verified the implementation and operation of the fractional step filters. It is clear from Tables 4 and 5 that actual fractional filter behavior has closely followed the theoretical one.

References

[1] M.D. Ortigueira, J.T.M. Machado, and P. O. Stalczyk, "Fractional signals and systems". *Bull. Pol. Ac.: Tech.* 66(4), 385–388 (2018).

[2] A. Dzielinski, D. Sierociuk, and G. Sarwas, "Some applications of fractional order calculus". *Bull. Pol. Ac.: Tech.* 58(4), 583–592 (2010).

[3] I. Podlubny, I. Petras, B. Vinagre, P. O'Leary, and L. Dorcak, "Analog realization of fractional – order controllers and nonlinear dynamics". *Nonlinear Dyn.* 29(1), 281–296 (2002).

[4] A. Acharya, S. Das, I. Pan, and S. Das, "Extending the concept of analog Butterworth filter for fractional order systems". *Signal Process.* 94, 409–420 (2014).

[5] A.M. Lopes and J.A.T. Machado, "Fractional-order model of a non-linear inductor". *Bull. Pol. Ac.: Tech.* 67(1), 61–67 (2019).

[6] R. Prasad, K. Kothari, and U. Mehta, "Flexible fractional supercapacitor model analyzed in time domain". *IEEE Access*, 7(1), 122 626–122 633 (2019).

[7] A. Radhwan, A. Elwakil, and A. Soliman, "On the generalization of second-order filters to the fractional order domain". *Journal of Circuits, Systems and Computers*, 18(2), 361–386 (2009).

[8] A. Ali, A. Radwan, and A. Soliman, "Fractional order Butterworth filter: Active and passive realizations". *IEEE J. Emerging Sel. Top. Circuits Syst.* 3(3), 346–354 (2013).

[9] T. Freeborn, A. Elwakil, and B. Maundy, "Approximated fractional-order inverse Chebyshev lowpass filters". *Circuits, Systems and Signal Process.* 35(6), 1973–1982 (2015).

[10] T. Freeborn, B. Maundy, and A. Elwakil, "Field programmable analogue array implementation of fractional step filters". *IET Circuits, Devices & Systems* 4(6), p. 514 (2010).

[11] D. Kubanek and T. Freeborn, "$(1 + \alpha)$ Fractional-order transfer functions to approximate low-pass magnitude responses with arbitrary quality factor". *Int. J. Electron. Commun.* 83, 570–578 (2018).

[12] T. Freeborn, "Comparison of $(1 + \alpha)$ fractional-order transfer functions to approximate lowpass Butterworth magnitude responses". *Circuits, Systems and Signal Process.* 35(6), 1983–2002 (2016).

[13] L.A. Said, S.M. Ismail, A.G. Radwan, A.H. Madian, M.F.A. El-Yazeed, and A.M. Soliman, "On the optimization of fractional order low-pass filters". *Circuits, Systems, and Signal Process.* 35(6), 2017–2039 (2016).

[14] S. Mahata, S.K. Saha, R. Kara, and D. Mandala, "Optimal design of fractional order low pass butterworth filter with accurate magnitude response". *Digital Signal Process.* 72, 96–114 (2018).

[15] F. Khateb, D. Kubanek, G. Tsirimokou, and C. Psychalinos, "Fractional-order filters based on low-voltage DDCCs". *Microelectron. J.*, 50, 50–59 (2016).

[16] J. Jerabek, R. Sotner, J. Dvorak, J. Polak, D. Kubanek, N. Herencsar, and J. Koton, "Reconfigurable fractional-order filter with electronically controllable slope of attenuation, pole frequency and type of approximation". *Journal of Circuits, Systems and Computers* 26(10), 1750–1757 (2017).

[17] G. Tsirimokou, C. Psychalinos, and A. Elwakil, *Design of CMOS analog integrated fractional-order circuits*. Springer: Switzerland, 2017.

[18] P. Ahmadi, B. Maundy, A.S. Elwakil, and L. Belostotski, "High-quality factor asymmetric-slope band-pass filters: a fractional-order capacitor approach". *IET Circuits, Devices & Systems* 6(3), 187 (2012).

[19] Y. Shi and R. C. Eberhart, "Empirical study of particle swarm optimization". in *Proceedings of the 1999 Congress on Evolutionary Computation-CEC99*, vol. 3, 1999.

[20] J. Kennedy and R. Eberhart, "Particle swarm optimization". in *IEEE International Conference on Neural Networks*, Perth, WA, 1995, pp. 1942–1948.

[21] D. Kubanek, T. Freeborn, J. Koton, and N. Herencsar, "Evaluation of $(1 + \alpha)$ fractional order approximated Butterworth high pass and band pass filter transfer functions". *Elektronika i Elektrotechnika* 24(2), 37–41 (2018).

[22] A. Radwan, A. Soliman, A. Elwakil, and A. Sedeek, "On the stability of linear systems with fractional-order elements". *Chaos, Solitons & Fractals* 40(5), 2317–2328 (2009).

[23] Anadigm, "3rd generation dynamically reconfigurable dpASP". *AN231E04 Datasheet Rev 1.2*, (2007).

[24] B. Krishna and K. Reddy, "Active and passive realization of fractance device of order 1/2". *Act. Passive Electron. Compon.* 1, 1–5 (2008).